

# Extended transient-grating self-referenced spectral interferometry for sub-100 nJ femtosecond pulse characterization

Xiong Shen (申雄)<sup>1</sup>, Jun Liu (刘军)<sup>1,2,\*</sup>, Fangjia Li (李方家)<sup>1,3</sup>, Peng Wang (王鹏)<sup>1</sup>,  
and Ruxin Li (李儒新)<sup>1,2</sup>

<sup>1</sup>State Key Laboratory of High Field Laser Physics, Shanghai Institute of Optics and Fine Mechanics,  
Chinese Academy of Sciences, Shanghai 201800, China

<sup>2</sup>IFSA Collaborative Innovation Center, Shanghai Jiao Tong University, Shanghai 200240, China

<sup>3</sup>Tongji University, Shanghai 200092, China

\*Corresponding author: jliu@siom.ac.cn

Received March 25, 2015; accepted May 27, 2015; posted online June 25, 2015

A geometry of transient-grating self-referenced spectral interferometry (TG-SRSI) is proposed for weak femtosecond pulse characterization. By using a reflective microscope objective (RMO), we build a compact, robust, and easy to adjust device with a higher sensitivity to pulse energy in comparison to all previous SRSI methods. A 65 nJ/ ~ 40 fs/1 kHz pulse at 800 nm is successfully characterized, which speaks to the capability of our device to characterize a weak pulse. It is expected to extend the TG-SRSI method to the characterization of femtosecond pulses from oscillators in the near future.

OCIS codes: 190.4380, 230.0040, 320.7100.

doi: 10.3788/COL201513.081901.

Self-referenced spectral interferometry (SRSI) has turned out to be a linear, analytical, accurate, and sensitive method to measure the full time-dependent intensity and phase of femtosecond pulses<sup>[1]</sup>. Compared to the two most widely used femtosecond pulse measurement methods, frequency-resolved optical gating (FROG)<sup>[2]</sup> and spectral phase interferometry for direct electric-field reconstruction<sup>[3]</sup>, SRSI has the advantage of using a straightforward algorithm based on the fast Fourier transform spectral interferometry (FTSI) process is to retrieve the spectral phase<sup>[1,4]</sup>. Non-linear frequency conservation effects, specifically, the cross-polarized wave generation (XPW)<sup>[1,5]</sup>, the self-diffraction (SD)<sup>[6]</sup>, and the transient grating (TG)<sup>[7]</sup> have been used in the SRSI method for femtosecond pulse characterization. Among them, XPW has a collinear and compact apparatus, but the use of polarizers limits the spectral range and pulse duration of the pulse to be characterized because of the dispersion and the limited spectral range introduced by the polarizers<sup>[8]</sup>. SD avoids the use of polarizers, but the non-collinear geometry makes the system complicated and introduces angular dispersion due to phase matching<sup>[6]</sup>. The TG process is self-phase matched at all wavelengths, background free, and alignment free, since the TG signal is generated in a unique direction different from the three input beams, but the same as the direction of the testing beam<sup>[7]</sup>. With no spectrum-sensitive optics such as a nonlinear crystal or polarizer, TG-SRSI has the potential to measure few-cycle pulses or even single-cycle pulses from the deep-UV to the mid-IR range with the appropriate spectrometers<sup>[7]</sup>.

It should be noted that XPW, SD, and TG are all four-wave mixing processes, which the third-order nonlinear

optical effects. Thus, the requirement of the incident pulse energy is relatively higher than that of the second-order nonlinear effect. Usually, a microjoule-level incident pulse is needed to obtain signals in both the XPW and SD<sup>[9]</sup> processes. As a result, the XPW- and SD-based SRSI methods can only measure femtosecond pulses with pulse energy at the microjoule level<sup>[1,4,6]</sup>. This property limits the application of the SRSI method to the characterization of weak femtosecond pulses, such as pulses from oscillators, which usually have pulse energies ranging from a few nanojoules to tens of nanojoules. Fortunately, it is found that the threshold for the TG effect is far below that of the SD and XPW effects, based on the results of the studies of FROG<sup>[9]</sup>. That is to say, TG-SRSI has the potential to characterize a weak femtosecond pulse.

In this Letter, we introduce an extremely simple SRSI device based on TG beam geometry for weak femtosecond pulse characterization. With the use of a key element reflective microscope objective (RMO), the device is compact, robust, easy to adjust, and has an extremely high sensitivity to pulse energy. As a proof-of-principle experiment, 43 fs/1 kHz input laser pulses at 800 nm with pulse energies ranging from 65 to 95 nJ are successfully characterized with the device, which verifies the ability of the device to characterize a weak pulse. The second harmonic generation (SHG) based FROG is used to measure the same pulse for comparison.

The TG process is popularly used in ultrashort pulse characterization and some nonlinear laser spectroscopy<sup>[9-12]</sup>. As TG is a third-order nonlinear optical effect, the generated TG signal has a cubic dependence on the time-dependent intensity of the three input pulses. The

expression of the TG signal can be written in the following way based on<sup>[9]</sup>:

$$I_{\text{TG}}(\Omega, t) \propto \left| \iint d\omega' d\omega'' E_1(t, \omega') E_2^*(t, \omega'') E_3(t, \Omega - \omega'' + \omega') \right|^2. \quad (1)$$

From the expression, it can be seen that the generated TG signal is smoothed and broadened due to the spectral integration of the three incident pulses, which are broader and smoother than the incident pulse<sup>[9]</sup>. As a result, it can be used for the reference beam in the SRSI method.

It can be seen that the intensity of the three incident pulses is the main parameter affecting the intensity of the TG signal. Thus, the first direct way to increase the intensity of the three weak incident pulses is to focus them more tightly. A RMO is used in our setup. Our geometry for the TG-SRSI is illustrated in Fig. 1(a). Usually, the setup is based on the BOXCARS beam geometry<sup>[7,13]</sup>. With this geometry, it turns out that the generated TG signal has a negligible angular dispersion<sup>[7]</sup>. In our case, the input beam is regarded as consisting of four identical beams: 1, 2, 3, and 4. A special coated glass plate is used to introduce a suitable attenuation of beam 4 and a suitable optical delay  $\tau$  between beam 4 and the other three beams. Then, the RMO focuses the four beams into a thin, nonlinear material. Beams 1, 2, and 3 are overlapped at the same time with the BOXCARS beam geometry, leading the self-phase matching according to the BOXCARS phase matching, as shown in Fig. 1(b). The TG signal is generated in the exact same direction as beam 4, the test beam, which makes the geometry alignment free and background free.

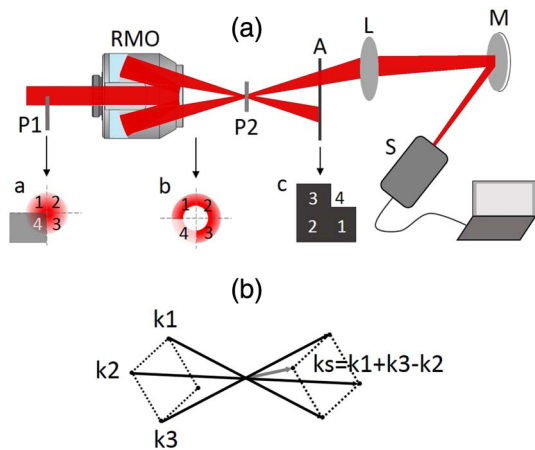


Fig. 1. (a) The optical setup of the RMO based TG-SRSI. P1, aluminum-coated, fused silica plate; P2, nonlinear material; A, black plate; L, lens; M, reflective plane mirror; S, spectrometer; a and b are cross sections of the portions indicated by the arrows and c is the black plate. All are seen from the right side. (b) BOXCARS phase-matching geometry.

The TG signal can be simply expressed as

$$E_{\text{TG}}(\omega) \propto E_1(\omega) E_2^*(\omega) E_3(\omega) = E_{\text{in}}^2(\omega) E_{\text{in}}^*(\omega), \quad (2)$$

where  $E_l(\omega)$  ( $l = 1, 2, 3$ ) represent incident beams 1, 2, and 3. We assume they are identical except for their directions during the focusing, which can be expressed as  $E_l(\omega) = E_{\text{in}}(\omega)$ . A spectral interferogram between the TG signal and test beam 4 can then be detected by a spectrometer. The detected spectral interferogram can be expressed as follows:

$$\begin{aligned} D(\omega, \tau) &= |E_{\text{TG}}(\omega) + E(\omega) e^{i\omega\tau}|^2 \\ &= |E_{\text{TG}}(\omega)|^2 + |E(\omega)|^2 \\ &\quad + E_{\text{TG}}^*(\omega) E(\omega) e^{i\omega\tau} + E_{\text{TG}}(\omega) E^*(\omega) e^{-i\omega\tau}. \end{aligned} \quad (3)$$

Here,  $S_0(\omega) = |E_{\text{TG}}(\omega)|^2 + |E(\omega)|^2$  is the sum of the spectra of the TG signal and incident beam 4, and  $f(\omega) = E_{\text{TG}}^*(\omega) E(\omega)$  is the interference part of the two laser pulses. Then, the spectral intensity and the spectral phase of the test beam can be obtained through several analytical calculation steps using the FTSI process with the same algorithm as<sup>[1,4,6]</sup>. Therefore, the temporal profile of the test beam can be completely characterized.

The RMO (LMM-15X-UVV) used here is a commercial product from Thorlabs. It consists of a concave mirror and a convex mirror; both of the mirrors are aluminum coated with about 83% reflectance at the central wavelength of 800 nm. There is an entrance pupil with an 8 mm diameter in the center of the concave mirror. The incident beam is guided into the RMO through the pupil. The convex mirror, together with its holder, will block the center of the incident beam. According to the parameter of the RMO, the ratio of the obscured area to the unobscured area is about 25%. Thus, the total transmittance of the RMO is about 41%. P1 is an aluminum-coated, 0.5 mm-thick fused silica plate that introduces an optical delay  $\tau$  of about 750 fs and about 99.5% of the energy attenuation of beam 4. The nonlinear material P2 is a 0.5 mm-thick fused silica plate. The obtained TG signal combined with the test beam are focused into a spectrometer (HR 4000 Ocean Optics) by using a lens with a 75 mm focal length and an aluminum-coated, highly reflective plane mirror.

A 1 kHz femtosecond pulse train at 800 nm from a chirped-pulse-amplification Ti:sapphire laser system (Coherent's Legend Elite Series) is used for the proof-of-principle experiment. The RMO's entrance pupil, which has a diameter of 8 mm, selects the center of the 10 mm diameter input beam for the measurement. The RMO, which has a focal length of about 13.3 mm, is extremely useful in characterizing the weak pulse. First, the short focal length yields a focal spot diameter of about 15  $\mu\text{m}$ . The 65 nJ/43 fs incident pulse has an intensity as high as 0.7 TW/cm<sup>2</sup>, which leads to our device being highly sensitivity to the incident pulse energy. Second, it utilizes a relatively larger part of the incident laser beam for the TG process in comparison to the TG-SRSI geometry proposed

by Liu *et al.*<sup>[7]</sup>. Third, it makes the setup extremely simple and compact.

The spectra of the testing beam, the TG signal, and the spectral interferogram are obtained independently by a spectrometer, and are shown in Fig. 2(a). It can be clearly seen that the spectrum of the TG signal is smoother and broader than that of the test beam. The intensity of the test beam is set to be lower than that of the TG signal by adjusting P1 so as to clearly distinguish the TG signal from the test beam in the calculation and reduce the calculation error. If the intensity of the test beam is too weak, a new coated fused silica plate (P1) with a lower reflectance is needed to reduce the intensity of the TG signal by using an appropriate iris to decrease the incident pulse energy. On the contrary, if the intensity of the test beam is too strong, P1 can be rotated to decrease its intensity.

The laser spectrum is obtained based on the spectral interferogram obtained by the spectrometer. It agrees well with the spectrum of the test beam obtained directly by the spectrometer, as shown in Fig. 2(b). At the same time, the spectral phase of the test beam is also retrieved. To check the reliability of our measurement, the output beam of the Ti:sapphire laser system is split into two beams using a splitter. The reflected light is used for our TG-SRSI measurement, and the transmission light is used for a homemade SHG-FROG measurement. Based on the measured FROG trace, we obtain the laser spectrum and spectral phase with a retrieved error smaller than 0.005 by using a commercial FROG software, which is also shown in Fig. 2(b). The spectra retrieved with the two methods have the same spectral bandwidth of about 26 nm, which are a little bit narrower than that of the test beam. This difference may be caused by the fluctuation of the test beam, leading to a relatively flat spectrum top. Figure 2(b) also shows the similarities in the retrieved spectral phases for both methods. The retrieved temporal profiles of the two methods are shown in Fig. 2(c). The pulse duration obtained with both methods are the same, about 43 fs, and their temporal phases are in good agreement with each other. The result loudly confirms the reliability of our geometry.

Figure 2(d) shows the three spectra of the TG signals from the bottom to the top that are measured directly by using the spectrometer with an integration time of 200 ms. They correspond to the input pulse energies of 65, 75, and 85 nJ. With our TG-SRSI geometry, we can obtain a smooth and broad TG signal spectrum even when the input pulse energy is as low as 65 nJ. This shows the ability of our device to characterize weak energy pulses. As the transmittance of the RMO is about 41%, only 27 of the 65 nJ of the input pulse are focused into the nonlinear material and take part in the TG signal generation process. With a longer integration time, a lower energy pulse can be characterized with the device. As the intensity of the TG signal can be calculated by the integral of its spectral intensity, as shown in Fig. 2(d), we can roughly obtain the ratio of the intensities of different TG signals by comparing the maximum normalized spectrum intensity of

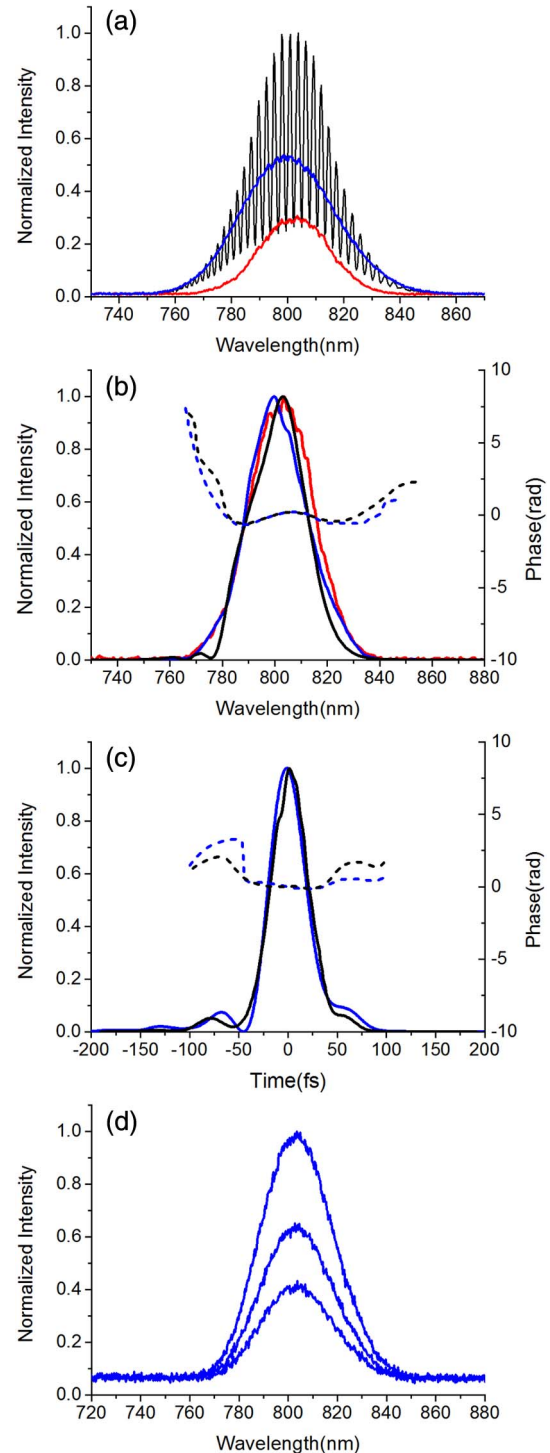


Fig. 2. (a) Spectral intensity of the test beam (red curve), the TG signal (blue curve), and the interference between them (black curve) measured directly with the spectrometer. (b) The spectrum retrieved (black solid curve) and the spectral phase (black dotted curve) by using TG-SRSI. The spectrum retrieved (blue solid curve) and the spectral phase retrieved (blue dotted curve) by using SHG-FROG. The red curve is the spectrum of the test beam measured directly by the spectrometer. (c) The temporal profiles (solid curves) and phases (dashed curves) retrieved by using TG-SRSI (black curves) and SHG-FROG (blue curves). (d) Spectra of three TG signals measured directly by the spectrometer. Spectra from the bottom to the top correspond to when the input pulse energies are 65, 75, and 85 nJ, respectively.

each TG signal. Thus, for the 65, 75, and 85 nJ input pulses, the intensity ratios of the TG signals are  $0.43:0.65:1 = 1:1.50:2.31 = H$ , while the intensity ratios of the incident pulses are  $65^3:75^3:85^3 = 1:1.53:2.24 = G$ ,  $H \approx G$ , which keeps the relationship between the TG signal and the input pulse as  $I_{TG} \propto I_{in}^3$ . The result also proves the reliability of our device from another aspect.

Can our device be extended to the characterization of femtosecond pulses from oscillators that have pulse energies of several nanojoules or tens of nanojoules? The answer is yes. At first, it needs to be noted that multi-shot energy sensitivity of the TG effect has been  $\sim 10$  nJ when 800 nm/100 fs pulses from an unamplified or regenerative amplified oscillator are focused to about 100  $\mu\text{m}$  in a non-linear medium<sup>[2,9]</sup>. Second, there are still several improvements that can be done in the near future to decrease the requirement of the incident pulse energy: 1) With a silver-coated-mirror-based RMO, the transmittance will be increased by about 1.3 times. 2) In the experiment, the RMO is a  $15\times$ , 0.30 NA objective. By using a  $40\times$ , 0.50 NA RMO, the focal spot will be much smaller. As  $I_{TG} \propto 1/d_{in}^6$ , this will increase the incident pulse energy sensitivity. 3) A 0.5 mm-thick fused silica glass is used in the proof-of-principle experiment. With a higher third-order susceptibility material, for example As<sub>2</sub>S<sub>3</sub>, Ge-S, or As-S-Ge<sup>[14]</sup>, the third-order susceptibility of which are two or three orders higher than that of the fused silica glass, the input pulse energy sensitivity will also be increased for the measurement. In all, several nanojoules pulses with megahertz repetition rates output from the laser oscillators can also be characterized directly using this device in the future.

In conclusion, we propose a geometry of TG-SRSI for pulse characterization. With the use of a key optical element, a RMO, our geometry is compact, robust, easy to adjust, and has an extremely high sensitivity to pulse energy compared to other SRSI devices. A 65 nJ pulse (27 nJ on the glass plate) is successfully characterized, which speaks to the ability of our device to characterize a weak pulse characterization. The result also agrees well

with that measured using the SHG-FROG, which proves the reliability of our geometry. This device is expected to characterize even several nanojoules of megahertz pulses from oscillators directly in the future.

This work was supported by the National Natural Science Foundation of China (Nos. 61178006, 11274327, and 61221064), the Shanghai Pujiang Program (No. 12PJ1409300), and the Recruitment Program of Global Experts.

## References

1. T. Oksenhendler, S. Coudreau, N. Forget, V. Crozatier, S. Grabielle, R. Herzog, O. Gobert, and D. Kaplan, *Appl. Phys. B* **99**, 7 (2010).
2. R. Trebino, K. W. DeLong, D. N. Fittinghoff, J. N. Sweetser, M. A. Krumbugel, B. A. Richman, and D. J. Kane, *Rev. Sci. Instrum.* **68**, 3277 (1997).
3. C. Iaconis and I. A. Walmsley, *Opt. Lett.* **23**, 792 (1998).
4. T. Oksenhendler, "Self-referenced spectral interferometry theory," <http://arxiv-web3.library.cornell.edu/abs/1204.4949> (April 22, 2012).
5. A. Moulet, S. Grabielle, C. Cornaggia, N. Forget, and T. Oksenhendler, *Opt. Lett.* **35**, 3856 (2010).
6. J. Liu, Y. Jiang, T. Kobayashi, R. Li, and Z. Xu, *J. Opt. Soc. Am. B* **29**, 29 (2012).
7. J. Liu, F. J. Li, Y. L. Jiang, C. Li, Y. X. Leng, T. Kobayashi, R. X. Li, and Z. Z. Xu, *Opt. Lett.* **37**, 4829 (2012).
8. A. Jullien, L. Canova, O. Albert, D. Boschetto, L. Antonucci, Y. H. Cha, J. P. Rousseau, P. Chaudet, G. Cheriaux, J. Etchepare, S. Kourtev, N. Minkovski, and S. M. Saitiel, *Appl. Phys. B* **87**, 595 (2007).
9. R. Trebino, *Frequency-Resolved Optical Gating: The Measurement of Ultrashort Laser Pulses* (Kluwer Academic Publishers, 2000).
10. J. N. Sweetser, D. N. Fittinghoff, and R. Trebino, *Opt. Lett.* **22**, 519 (1997).
11. D. W. Phillion, D. J. Kuizenga, and A. E. Siegman, *Appl. Phys. Lett.* **27**, 85 (1975).
12. H. J. Eichler, U. Klein, and D. Langhans, *Appl. Phys.* **21**, 215 (1980).
13. A. C. Eckbreth, *Appl. Phys. Lett.* **32**, 421 (1978).
14. A. R. Molla, A. Tarafder, S. Mukherjee, and B. Karmakar, *Opt. Mater. Express* **4**, 843 (2014).